Image Reconstruction of a Complex Cylinder Illuminated by TE Waves

Chien-Ching Chiu and Po-Tsun Liu

Abstract—**The electromagnetic inverse scattering of a complex cylinder illuminated by transverse electric (TE) waves is investigated. The complex cylinder is a conductor coated by dielectric materials. A group of various unrelated TE waves is incident upon the object and the scattered fields are measured outside. With prior knowledge of the conductor's shape, the complex permittivity distribution of the dielectric materials can be reconstructed. The algorithm is based on the moment method and the unrelated illumination method. Some numerical examples are given to demonstrate the capability of the algorithm. Numerical results show that the dielectric constant and the conductivity distribution of the materials can be reconstructed even when the scattered fields are contaminated by random Gaussian noise.**

I. Introduction

THE INVERSE scattering problem is to reconstruct the shape or the dielectric constant of an unknown scatterer from the scattering data measured outside. This problem has attracted increasing attention owing to interests in remote sensing, medical imaging, and nondestructive evaluation. Generally speaking, two categories of approaches have been developed for the inverse scattering problem. This first is the approximate approach, such as the physical optics method [1]–[3], the Born and the Rytov approximations [4]–[6]. The inverse problem can be simplified if some approximations are properly applied. However, there are limitations on these approximations [1]–[6]. The second approach is to solve the exact equations rigorously by numerical methods [7]–[14]. The rigorous one does not need approximation in formulation, but its computation is more complicated than the approximate one. Besides, most papers for two-dimensional (2-D) inverse problem with the rigorous approach are dealt with TM wave illumination because the vectorial problem can be simplified to a scalar one. Two-dimensional inverse problem for the TE waves is scarce [15], [16]. Based on the Newton–Kantorovitch method, an iterative algorithm to reconstruct the permittivities of a dielectric object was proposed by Joachimowicz *et al.* [15]. Otto and Chew developed the local shape-function algorithm for the imaging of dielectric objects illuminated by the TE waves. They used the T-matrix formulation instead of standard integral equation method [16].

In this paper, the electromagnetic imaging of a complex cylinder illuminated by TE waves is investigated. The complex cylinder is a conductor coated with dielectric materials. By the knowledge of the conductor's shape and the scattered field measured outside, the permittivity distribution of the dielectric materials has been reconstructed. This method is potentially important in medical imaging and biological applications. In Section II, the theoretical formulation is presented. Numerical results are given in Section III. Finally some conclusions are drawn in Section IV.

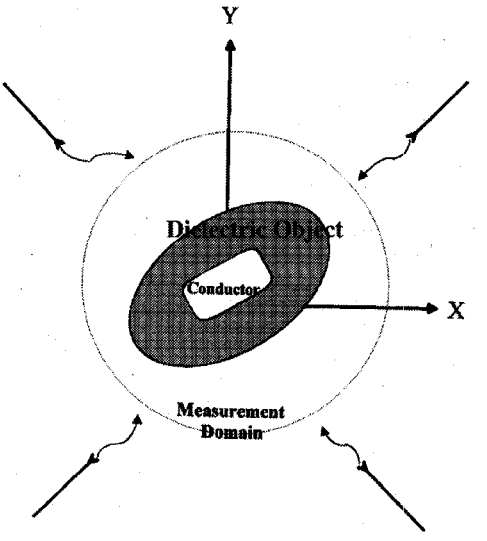

Fig. 1. Geometry of the problem in the (x, y) plane.

II. Theoretical Formulation

Fig. 1 shows the geometry of the problem. A conductor coated by dielectric materials located in the free space is infinitely extended in the z-direction. The relative complex permittivity ϵ_c can be expressed as

$$\epsilon_c(x, y) = \epsilon_r(x, y) - j\frac{\sigma(x, y)}{\omega\epsilon_0}.$$

Note that the $e^{j\omega t}$ time dependence is assumed for the formulation.

Incident waves with the electric field polarized in the x-y plane, i.e., transverse electric (TE) waves, is incident upon the object. Owing to the added difficulty of induced polarization charges, this vectorial problem cannot simplified into a scalar one. Thus the equivalent current concept and Hertz vectorial potential techniques are employed to solve the problem. The integral equation for the field inside the materials can be

Manuscript received October 1, 1995; revised March 11, 1996. This work was supported by the National Science Council, Republic of China, Grant NSC 85-2213-E032-001.

The authors are with the Department of Electrical Engineering, Tamkang University, Tamsui, Taiwan, ROC.

Publisher Item Identifier S 0018-9480(96)07018-4.

expressed as follows [17], [18]:

$$-E_x^i(\bar{r}) = \left(\frac{\partial^2}{\partial x^2} + k_0^2\right)\left[\int_s G(\bar{r}, \bar{r}')(\epsilon_c(\bar{r}') - 1)E_x(\bar{r}')ds'\right] + \frac{\partial^2}{\partial x \partial y}\left[\int_s G(\bar{r}, \bar{r}')(\epsilon_c(\bar{r}') - 1)E_y(\bar{r}')ds'\right] + \frac{\partial}{\partial y}\left[\int_c G(\bar{r}, \bar{r}')M_s(\bar{r}')dl'\right] - E_x(\bar{r}) - E_y^i(\bar{r}) \quad (1)$$

$$= \frac{\partial^2}{\partial x \partial y}\left[\int_s G(\bar{r}, \bar{r}')(\epsilon_c(\bar{r}') - 1)E_x(\bar{r}')ds'\right] + \left(\frac{\partial^2}{\partial y^2} + k_0^2\right)\left[\int_s G(\bar{r}, \bar{r}')(\epsilon_c(\bar{r}') - 1)E_y(\bar{r}')ds'\right] - \frac{\partial}{\partial x}\left[\int_c G(\bar{r}, \bar{r}')M_s(\bar{r}')dl'\right] - E_y(\bar{r}) \quad (2)$$

where E_x^i and E_y^i are the x and y components of the incident field, respectively. E_x and E_y are the x and y components of the total field, respectively. M_s is the equivalent magnetic surface current density in the z direction. $G(\bar{r}, \bar{r}')$ is 2-D Green function for free space

$$G(\bar{r}, \bar{r}') = -\frac{j}{4}H_0^{(2)}(k_0|\bar{r} - \bar{r}'|).$$

Here $H_0^{(2)}$ stands for the Hankel function of the second kind of the zeroth order.

Since the tangential components of $\overline{E}$ on the surface of the perfect conductor should be zero, one can obtain the following integral equation:

$$-\hat{n}\times(E_x^i(\bar{r})\hat{x} + E_y^i(\bar{r})\hat{y}) = \hat{n} \times \left\{\left[\left(\frac{\partial^2}{\partial x^2} + k_0^2\right) \cdot \left[\int_s G(\bar{r}, \bar{r}')(\epsilon_c(\bar{r}') - 1)E_x(\bar{r}')ds'\right] + \frac{\partial^2}{\partial x \partial y}\left[\int_s G(\bar{r}, \bar{r}')(\epsilon_c(\bar{r}') - 1)E_y(\bar{r}')ds'\right] + \frac{\partial}{\partial y}\int_c G(\bar{r}, \bar{r}')M_s(\bar{r}')dl'\right]\hat{x} + \left[\frac{\partial^2}{\partial x \partial y}\left[\int_s G(\bar{r}, \bar{r}')(\epsilon_c(\bar{r}') - 1)E_x(\bar{r}')ds'\right] + \left(\frac{\partial^2}{\partial y^2} + k_0^2\right)\left[\int_s G(\bar{r}, \bar{r}')(\epsilon_c(\bar{r}') - 1)E_y(\bar{r}')ds'\right] - \frac{\partial}{\partial x}\int_c G(\bar{r}, \bar{r}')M_s(\bar{r}')dl'\right]\hat{y}\right\} \quad (3)$$

where $\hat{n}$ is the outward unit vector normal to the surface of the conductor. The scattered field outside the scatterer can be expressed by

$$E_r^s(\bar{r}) = \left(\frac{\partial^2}{\partial x^2} + k_0^2\right)\left[\int_s G(\bar{r}, \bar{r}')(\epsilon_c(\bar{r}') - 1)E_x(\bar{r}')ds'\right] + \frac{\partial^2}{\partial x \partial y}\left[\int_s G(\bar{r}, \bar{r}')(\epsilon_c(\bar{r}') - 1)E_y(\bar{r}')ds'\right] + \frac{\partial}{\partial y}\left[\int_c G(\bar{r}, \bar{r}')M_s(\bar{r}')dl'\right] \quad (4)$$

$$E_y^s(\bar{r}) = \frac{\partial^2}{\partial x \partial y}\left[\int_s G(\bar{r}, \bar{r}')(\epsilon_c(\bar{r}') - 1)E_x(\bar{r}')ds'\right] + \left(\frac{\partial^2}{\partial y^2} + k_0^2\right)\left[\int_s G(\bar{r}, \bar{r}')(\epsilon_c(\bar{r}') - 1)E_y(\bar{r}')ds'\right] - \frac{\partial}{\partial x}\left[\int_c G(\bar{r}, \bar{r}')M_s(\bar{r}')dl'\right]. \quad (5)$$

In order to solve the direct problem for given $\epsilon_c(\bar{r})$ and conductor's shape, the moment method is applied. The dielectric materials are divided into N_1 sufficient small cells such that the total field and the permittivity can be considered constant in each cell. Similarly, the contour of the conductor is divided into N_2 sufficient segments. Thus the equivalent magnetic surface current density over each segment can be taken as constant. By employing the point-matching technique, (1)–(5) can be transformed into matrix equations

$$\begin{pmatrix} -E_x^i \\ -E_y^i \end{pmatrix} = \left\{\begin{bmatrix}[G_1] & [G_2] \\ [G_2] & [G_4]\end{bmatrix}\begin{bmatrix}[\tau] & 0 \\ 0 & [\tau]\end{bmatrix} - \begin{bmatrix}[I] & 0 \\ 0 & [I]\end{bmatrix}\right\}\begin{pmatrix} E_x \\ E_y \end{pmatrix} + \begin{bmatrix}[G_3] \\ [G_5]\end{bmatrix}(M_s) \quad (6)$$

$$-(E_h^i) = [G_6][\tau] + [G_7][\tau] + [G_8](M_s) \quad (7)$$

$$\begin{pmatrix} E_x^s \\ E_y^s \end{pmatrix} = \begin{bmatrix}[G_9] & [G_{10}] \\ [G_{10}] & [G_{12}]\end{bmatrix}\begin{bmatrix}[\tau] & 0 \\ 0 & [\tau]\end{bmatrix} \cdot \begin{pmatrix} E_x \\ E_y \end{pmatrix} + \begin{bmatrix}[G_{11}] \\ [G_{13}]\end{bmatrix}(M_s) \quad (8)$$

where (E_x^i) and (E_y^i) denote the N_1 element incident field column vectors. (E_x) and (E_y) are N_1 element total field column vectors. (E_h^i) represents the N_2 element incident column vector. (E_x^s) and (E_y^s) are the M element scattered field column vectors. Here M is the number of measurement points. (M_s) is the N_2 element column vector. The matrices $[G_1]$, $[G_2]$ and $[G_4]$ are $N_1 \times N_1$ square matrices. $[G_3]$ and $[G_5]$ are $N_1 \times N_2$ matrices. $[G_6]$ and $[G_7]$ are $N_2 \times N_1$ matrices. $[G_8]$ is a $N_2 \times N_2$ matrix. $[G_9]$, $[G_{10}]$ and $[G_{12}]$ are $M \times N_1$ matrices. $[G_{11}]$ and $[G_{13}]$ are $M \times N_2$ matrices. The elements in matrices $[G_i]$, $i = 1, 2, \ldots, 13$, can be computed by complex mathematic manipulation (see Appendix). $[\tau]$ is a $N_1 \times N_1$ diagonal matrix whose diagonal element $[\tau]_{nn}$ is equal to $(\epsilon_c)_{nn} - 1$. $[I]$ is a $N_1 \times N_1$ identity matrix. The direct problem can be solved by using matrix equations (6)–(8).

The inverse problem is, given the shape of the conductor and the measured scattered field, compute the permittivity distribution of the dielectric materials. To solve this problem, (M_s) in (7) is first computed and substituted into (6) and (8). Next we use $2N_1$ different incident column vectors to illuminate the object, the following equations are obtained:

$$-[E_t^i] = ([G_{t1}][\tau_t] - [I_t])[E_t] \quad (9)$$

$$[E_t^s] = [G_{t2}][\tau_t][E_t] \quad (10)$$

where

$$[E_t^i] = \begin{bmatrix} E_x^i - [G_3][G_8]^{-1}(E_h^i) \\ E_y^i - [G_5][G_8]^{-1}(E_h^i) \end{bmatrix}$$

$$[E_t^s] = \begin{bmatrix} E_x^s + [G_{11}][G_8]^{-1}(E_h^i) \\ E_y^s + [G_{13}][G_8]^{-1}(E_h^i) \end{bmatrix}$$

$$[E_t] = \begin{bmatrix} E_x \\ E_y \end{bmatrix}$$

$$[G_{t1}] = \begin{bmatrix} [G_1] - [G_3][G_8]^{-1}[G_6] & [G_2] \\ [G_2] & [G_4] - [G_5][G_8]^{-1}[G_7] \end{bmatrix}$$

$$[G_{t2}] = \begin{bmatrix} [G_9] - [G_{11}][G_8]^{-1}[G_6] & [G_{10}] \\ [G_{10}] & [G_{12}] - [G_{13}][G_8]^{-1}[G_7] \end{bmatrix}$$

$$[\tau_t] = \begin{bmatrix} [\tau] & 0 \\ 0 & [\tau] \end{bmatrix} \qquad [I_t] = \begin{bmatrix} [I] & 0 \\ 0 & [I] \end{bmatrix}.$$

Here $[E_t^i]$ and $[E_t]$ are both $2N_1 \times 2N_1$ matrices. $[E_t^s]$ is a $M \times 2N_1$ matrix. Note that the matrix $[G_8]$ is diagonally dominant and always invertible. It is worth mentioning that other than the matrix $[G_{t2}]$, the matrix $[G_{t1}][\tau_t] - [I_t]$ is always a well-posed one in any case. Therefore (9) can be rewritten as

$$[E_t] = -([G_{t1}][\tau_t] - [I_t])^{-1}[E_t^i]. \tag{11}$$

Substituting (11) into (10), we get

$$([E_t^s][E_t^i]^{-1}[G_{t1}] + [G_{t2}])[\tau_t] = [E_t^s][E_t^i]^{-1}.$$

If we use the following matrix notations:

$$[\phi_t] = [E_t^s][E_t^i]^{-1}$$
$$[\Psi_t] = [E_t^s][E_t^i]^{-1}[G_{t1}] + [G_{t2}].$$

Then $[\tau_t]$ can be found by solving the following equations:

$$[\Psi_t][\tau_t] = [\phi_t]. \tag{12}$$

From (12), all the diagonal elements in matrix $[\tau]$ can be determined by comparing the element with the same subscripts which may be any row of both $[\Psi_t]$ and $[\phi_t]$:

$$(\tau)_{nn} = \frac{(\phi_t)_{mn}}{(\Psi_t)_{mn}}, \; n \le N_1$$

or

$$(\tau)_{(n-N_1)(n-N_1)} = \frac{(\phi_t)_{mn}}{(\Psi_t)_{mn}}, \; n \ge N_1 + 1.$$

Then the permittivities of each cell can be obtained as follows:

$$\epsilon_n = (\tau)_{nn} + 1.$$

Note that there are a total of $2M$ possible values for each element of τ. Therefore, the average value of these $2M$ data is computed and chosen as final reconstruction result in the simulation.

In the above derivation, the key problem is that the incident matrices $[E_t^i]$ must not be a singular matrix, i.e., all the incident column vectors that form the $[E_t^i]$ matrices, must be linearly unrelated. Thus, if the object is illuminated by a group of unrelated incident wave, it is possible to reconstruct the permittivity distribution of the materials. Note that when the number of cells becomes very large, it is difficult to make such a great number of independent measurements. In such a case, some regularization methods must be used to overcome the ill-posedness.

III. Numerical Results

In this section, we report some numerical results obtained by computer simulations using the method described in Section II. Lossy dielectric materials coats on a perfectly conducting rod of different cross-sections are considered. The sensitivity of this method to random Gaussian noise in the scattered field is also investigated.

The frequency of the incident waves is chosen to be 3 GHz and the number of illuminations is the same as that of cells. The incident waves are generated by numerous groups of radiators operated, simultaneously. Each group of radiators is restricted to transmit a narrow bandwidth pattern which can be implemented by antenna array techniques. By changing the beam direction and tuning the phase of each group of radiators, one can focus all the incident beams in turn at each cell of the object. This procedure is named "beam focusing" [12]. Note that this focusing should be set when the scatterer is absent. Clearly, an incident matrix formed in this way is diagonally dominant and its inverse matrix exists. The measurement is taken on a circle of radius 0.1 m. For avoiding trivial inversion of finite-dimensional problems, the discretization number for the direct problem is four times as that for the inverse problem in our numerical simulation.

A 5 cm × 5 cm (1/2 wavelength × 1/2 wavelength) square rectangular cross-sections of a perfectly conducting rod coated with dielectric materials with rectangular cross-sections is our first example. The dielectric materials are discretized into 10×10 cells and their relative permittivities are plotted in Fig. 2. Each cells has a 0.5 cm × 0.5 cm cross section. The reconstructed results are shown in Fig. 3. Note that there are totally 768 data points being used for this example. The root mean square error is about 1.5% for the complex permittivity ϵ_c. It is apparent that the reconstruction is good.

In the second example, the circular cross-section of dielectric materials coated on a cylindrical conductor is discretized into 90 cells and their relative permittivities are plotted in Fig. 4. The radius of conductor and the dielectric materials are 1 cm and 2.5 cm (1/4 wavelength), respectively. The reconstructed results are shown in Fig. 5. Note that there are totally 1620 data points being used. The root mean square error is about 2.9% for the complex permittivity ϵ_c. We can see the reconstruction is also good.

To investigate the effects of noise on our inverse algorithm, we added Gaussian noise with zero mean to the real and imaginary parts of the simulated data. Normalized standard deviations of 0.001%, 0.01%, 0.1%, 1%, and 10% are used in

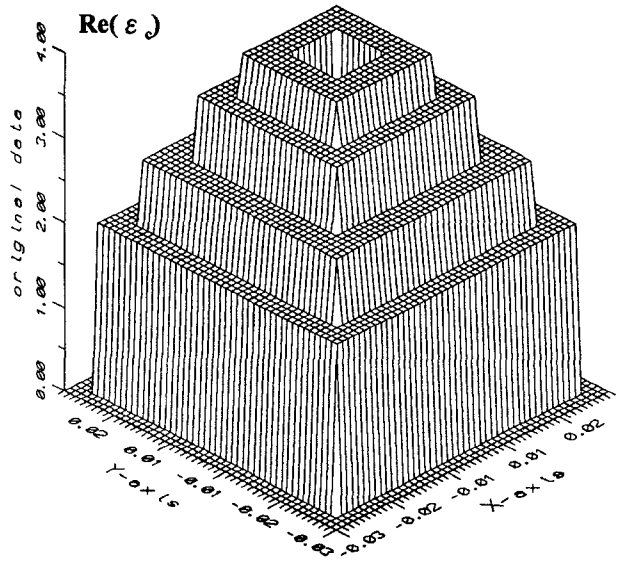

(a)

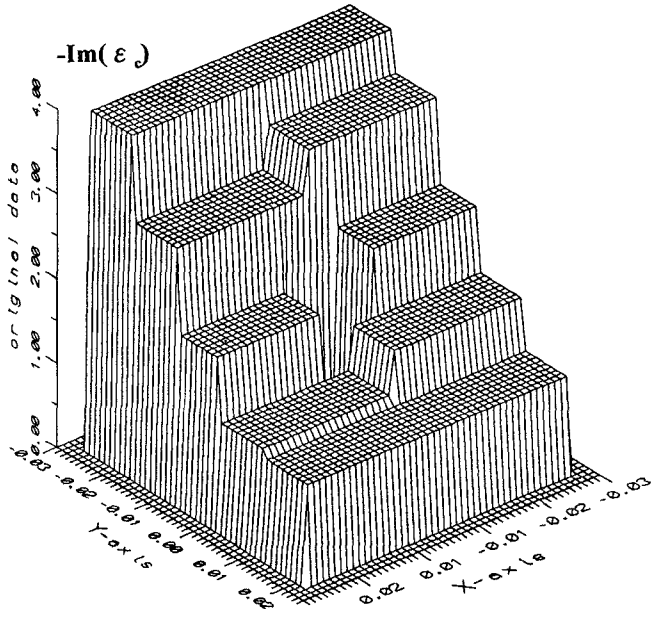

(b)

Fig. 2. Original complex relative permittivity distribution, $\epsilon_c(x, y)$, for example 1. (a) The real part of $\epsilon_c(x, y)$. (b) The imaginary part of $\epsilon_c(x, y)$.

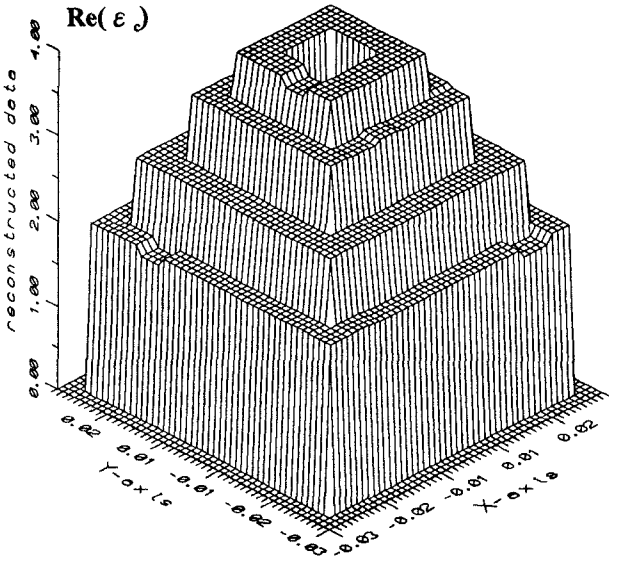

(a)

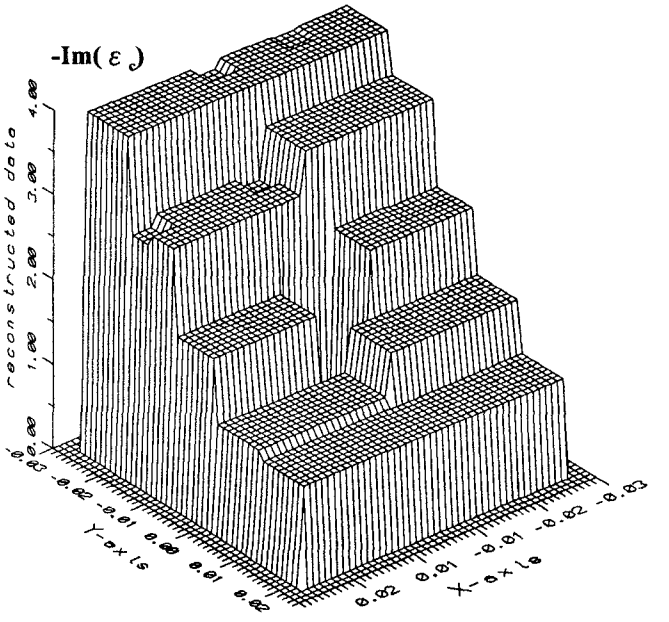

(b)

Fig. 3. Reconstructed complex relative permittivity distribution, $\epsilon_c(x, y)$, for example 1. (a) The real part of $\epsilon_c(x, y)$. (b) The imaginary part of $\epsilon_c(x, y)$.

the simulations. Note that the normalized standard deviation is defined as the standard deviation of the Gaussian noise divided by the root mean square value of the scattered field. The numerical results for example 1 and 2 are plotted in Fig. 6. We can see that the reconstruction is still good even 0.1% noise exists.

Our method depends on the condition number of $[E_t^i]$, i.e., on having $2N_1$ unrelated measurements. The procedure will generally not work when the number of unknowns gets very large. This is due to the fact that is is difficult to make such a great number of measurements and make them all unrelated. As a result, the condition number of $[E_t^i]$ will become large while the number of unknowns is very large. In such a case, the regularization method should be employed to overcome the illposedness. For instance, the singular value decomposition technique [8] can be applied for the inversion of the $[E_t^i]$ matrix.

IV. Conclusion

Imaging algorithm for the TE case is more complicated than that for the TM case, due to the added difficulties in the polarization charges. Nevertheless, the polarization charges cannot be ignored for this two-dimensional problem and all three-dimensional problems. In this paper, an efficient algorithm for imagine a complex cylinder, i.e., a conductor coated with dielectric materials, illuminated by TE waves, has been proposed. By properly arranging the direction of various

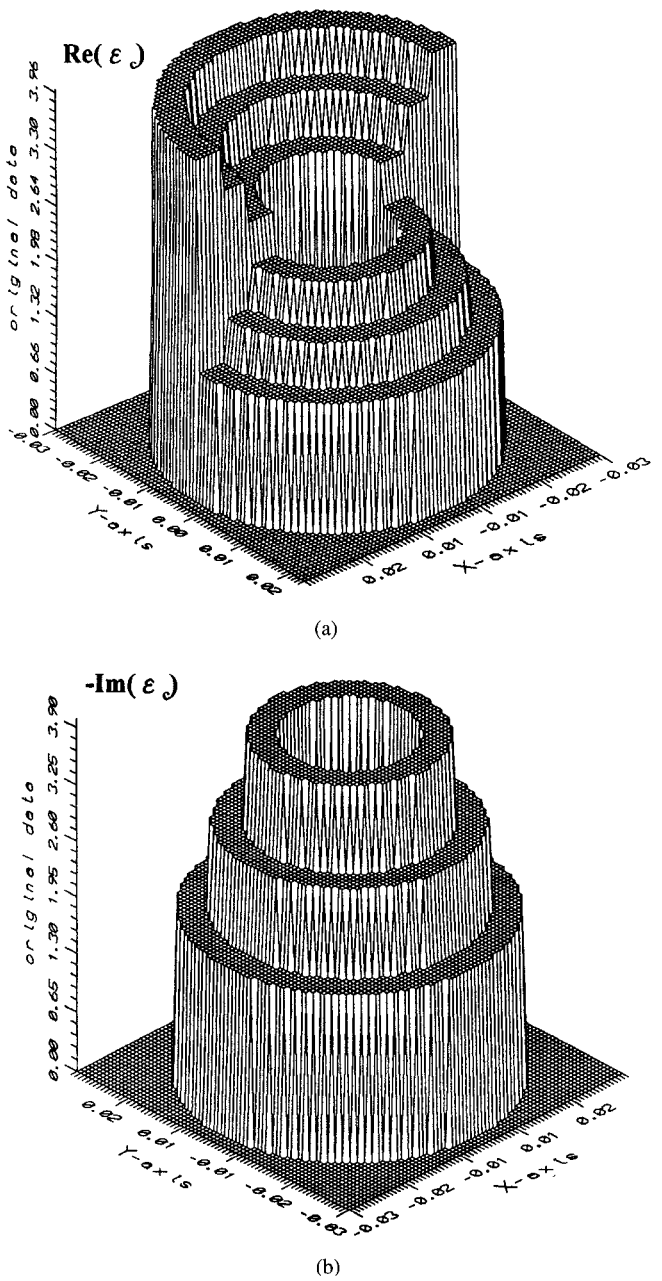

(a) (b)

Fig. 4. Original complex relative permittivity distribution, $\epsilon_c(x, y)$, for example 2. (a) The real part of $\epsilon_c(x, y)$. (b) The imaginary part of $\epsilon_c(x, y)$.

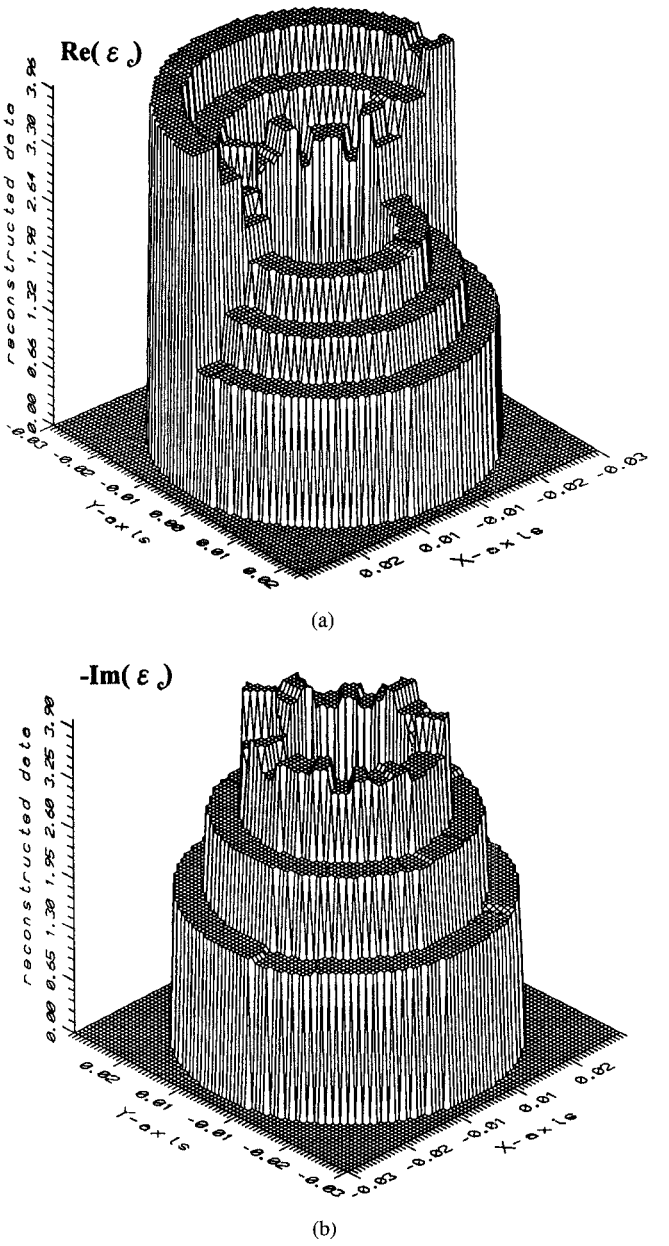

(a) (b)

Fig. 5. Reconstructed complex relative permittivity distribution, $\epsilon_c(x, y)$, for example 2. (a) The real part of $\epsilon_c(x, y)$. (b) The imaginary part of $\epsilon_c(x, y)$.

unrelated waves, the difficulty of illposedness and nonlinearity is avoided. Thus, the dielectric constant and the conductivity distribution can be obtained by simple matrix operations. This algorithm is very effective and efficient, since no iteration is required. The further research is the application of this method on the inverse problem of composite materials coated on the metal and aircraft.

APPENDIX

The element in the matrix $[G_1]$ can be written as

$$(G_1)_{mn} = -\frac{j}{4}\left(\frac{\partial^2}{\partial x^2} + k_0^2\right) \cdot \int\int_{\text{cell n}} H_0^{(2)}(k_0\sqrt{(x_m - x')^2 + (y_m - y')^2})dx'dy'$$

where (x_m, y_m) is the observation point located in the center of the mth cell. Note that the observation point is expressed as (x_m, y_m) in Cartesian coordinates and (r_m, θ_m) in polar coordinates. For a sufficient small cell, we can replace the cell by a circular cell with the same cross section [19]. Let the equivalent radius of the nth circular cell be a_n. Then $(G_1)_{mn}$ can be expressed in a simple analytic form

$$(G_1)_{mn} = \begin{cases} -\frac{j\pi a_n J_1(k_0 a_n)}{2\rho_{mn}^3}[k_0\rho_{mn}(y_m - y_n)^2 H_0^{(2)}(k_0\rho_{mn}) \\ \quad +((x_m - x_n)^2 - (y_m - y_n)^2)H_1^{(2)}(k_0\rho_{mn})], \\ \quad m \neq n \\ -\frac{1}{4}[\pi k_0 a_n H_1^{(2)}(k_0 a_n) - 4j], \qquad m = n \end{cases}$$

with $\rho_{mn}\sqrt{(x_m - x_n)^2 + (y_m - y_n)^2}$, where J_1 is Bessel function of the first kind of first order and (x_n, y_n) is the

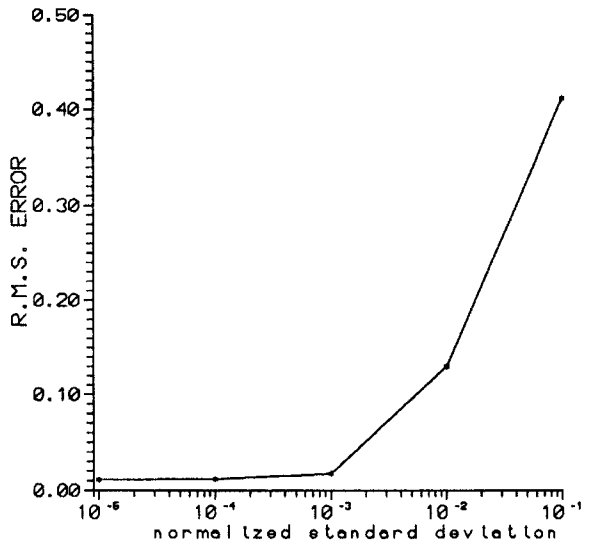

(a)

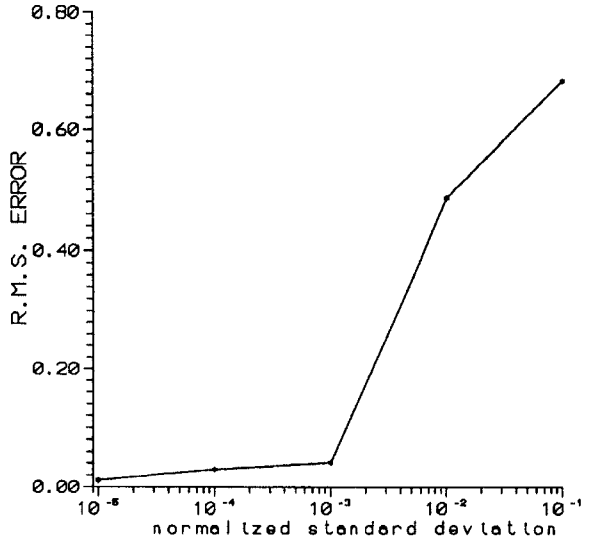

(b)

Fig. 6. Reconstruction error as a function of normalized standard deviation of Gaussian noise. (a) Example 1. (b) Example 2.

center of the cell n. Similarly

$$(G_2)_{mn} = \begin{cases} -\frac{j\pi a_n J_1(k_0 a_n)}{2\rho_{mn}^3}(x_m - x_n)(y_m - y_n) \\ \quad \cdot[2H_1^{(2)}(k_0\rho_{mn}) - k_0\rho_{mn}H_0^{(2)}(k_0\rho_{mn})], \\ \quad m \neq n \\ 0, \qquad m = n \end{cases}$$

$$(G_3)_{mn} = \frac{jk_0}{4}\Delta C_n \frac{y_m - y_n}{\rho_{mn}} H_1^{(2)}(k_0\rho_{mn})$$

with $\rho_{mn} = \sqrt{(x_m - x_n)^2 + (y_m - y_n)^2}$, where (x_n, y_n) is the center of the nth segment of the conductor's contour and ΔC_n denotes the nth segment of the conductor

$$(G_4)_{mn} = \begin{cases} -\frac{j\pi a_n J_1(k_0 a_n)}{2\rho_{mn}^3}[k_0\rho_{mn}(x_m - x_n)^2 \\ \quad \cdot H_0^{(2)}(k_0\rho_{mn}) \\ \quad +((y_m - y_n)^2 - (x_m - x_n)^2) \\ \quad \cdot H_1^{(2)}(k_0\rho_{mn})], & m \neq n \\ -\frac{j}{4}[\pi k_0 a_n H_1^{(2)}(k_0 a_n) - 4j], & m = n \end{cases}$$

$$(G_5)_{mn} = \frac{jk_0}{4}\Delta C_n \frac{-(x_m - x_n)}{\rho_{mn}} H_1^{(2)}(k_0\rho_{mn}).$$

Since the values of the elements in the matrices $[G_6]$, $[G_7]$, and $[G_8]$ depend on the conductor's shape, the following expressions of $[G_6]$, $[G_7]$ and $[G_8]$ are only valid for the conducting cylinder of circular cross section. It is straightforward to calculate the matrices corresponding to the conductor with different cross-section

$$\begin{aligned}(G_6)_{mn} = &-\sin(\theta_m)\left(-\frac{j\pi a_n J_1(k_0 a_n)}{2\rho_{mn}^3}\right. \\ &\cdot[k_0\rho_{mn}(y_m - y_n)^2 H_0^{(2)}(k_0\rho_{mn}) \\ &\left. + ((x_m - x_n)^2 - (y_m - y_n)^2)H_1^{(2)}(k_0\rho_{mn})]\right) \\ &+ \cos(\theta_m)\left(-\frac{j\pi a_n J_1(k_0 a_n)}{2\rho_{mn}^3}(x_m - x_n)\right. \\ &\cdot (y_m - y_n)[2H_1^{(2)}(k_0\rho_{mn}) \\ &\left. - k_0\rho_{mn}H_0^{(2)}(k_0\rho_{mn})]\right)\end{aligned}$$

$$\begin{aligned}(G_7)_{mn} = &-\sin(\theta_m)\left(-\frac{j\pi a_n J_1(k_0 a_n)}{2\rho_{mn}^3}(x_m - x_n)\right. \\ &\cdot (y_m - y_n)[2H_1^{(2)}(k_0\rho_{mn}) \\ &\left. - k_0\rho_{mn}H_0^{(2)}(k_0\rho_{mn})]\right) \\ &+ \cos(\theta_m)\left(-\frac{j\pi a_n J_1(k_0 a_n)}{2\rho_{mn}^3}\right. \\ &\cdot [k_0\rho_{mn}(x_m - x_n)^2 H_0^{(2)}(k_0\rho_{mn}) \\ &\left. + ((y_m - y_n)^2 - (x_m - x_n)^2)H_1^{(2)}(k_0\rho_{mn})]\right)\end{aligned}$$

$$(G_8)_{mn} = \begin{cases} \frac{jk_0}{4}\Delta C_n \frac{(x_n - x_m)\cos\theta_m + (y_n - y_m)\sin\theta_m}{\rho_{mn}} \\ \quad \cdot H_1^{(2)}(k_0\rho_{mn}), & m \neq n \\ \frac{jk_0^2 r_m^2}{4}\left[\sin\left(\frac{\Delta C_n}{2r_m}\right) - \frac{\Delta C_n}{2r_m}\right] + \frac{\Delta C_n}{4\pi r_m}, & m = n \end{cases}$$

$$\begin{aligned}(G_9)_{mn} = &-\frac{j\pi a_n J_1(k_0 a_n)}{2\rho_{mn}^3}[k_0\rho_{mn}(y_m - y_n)^2 H_0^{(2)}(k_0\rho_{mn}) \\ &+((x_m - x_n)^2 - (y_m - y_n)^2)H_1^{(2)}(k_0\rho_{mn})]\end{aligned}$$

$$(G_{10})_{mn} = -\frac{j\pi a_n J_1(k_0 a_n)}{2\rho_{mn}^3}(x_m - x_n)(y_m - y_n) \cdot [2H_1^{(2)}(k_0\rho_{mn}) - k_0\rho_{mn}H_0^{(2)}(k_0\rho_{mn})]$$

$$(G_{11})_{mn} = \frac{jk_0}{4}\Delta C_n \frac{(y_m - y_n)}{\rho_{mn}} H_1^{(2)}(k_0\rho_{mn})$$

$$(G_{12})_{mn} = -\frac{j\pi a_n J_1(k_0 a_n)}{2\rho_{mn}^3}[k_0\rho_{mn}(x_m - x_n)^2 \cdot H_0^{(2)}(k_0\rho_{mn}) + ((y_m - y_n)^2 - (x_m - x_n)^2) \cdot H_1^{(2)}(k_0\rho_{mn})]$$

$$(G_{13})_{mn} = \frac{jk_0}{4}\Delta C_n \frac{-(x_m - x_n)}{\rho_{mn}} H_1^{(2)}(k_0\rho_{mn}).$$

REFERENCES

[1] R. M. Lewis, "Physical optics inverse diffraction," *IEEE Trans. Antennas Propagat.,* vol. 17, pp. 308–314, May 1969.

[2] T. H. Chu and N. H. Farhat, "Polarization effects in microwave diversity imaging of perfectly conducting cylinders," *IEEE Trans. Antennas Propagat.,* vol. 37, pp. 235–244, Feb. 1989.

[3] D. B. Ge, "A study of the Lewis method for target-shape reconstruction," *Inverse Problems,* vol. 6, pp. 363–370, June 1990.

[4] J. B. Keller, "Accuracy and validity of Born and Rytov approximations," *J. Opt. Soc. Am.,* vol. 59, pp. 1003–1004, 1969.

[5] M. Slaney, A. C. Kak, and L. E. Larsen, "Limitations of imaging with first-order diffraction tomography," *IEEE Trans. Microwave Theory Tech.,* vol. 32, pp. 860–874, Aug. 1984.

[6] T. H. Chu, "Polarization effects on microwave imaging of dielectric cylinder," *IEEE Trans. Microwave Theory Tech.,* vol. 36, pp. 1366–1369, Sept. 1988.

[7] A. Roger, "Newton–Kantorovitch algorithm applied to an electromagnetic inverse problem," *IEEE Trans. Antennas Propagat.,* vol. 29, pp. 232–238, Mar. 1981.

[8] W. Tobocman, "Inverse acoustic wave scattering in two dimensions from impenetrable targets," *Inverse Problems,* vol. 5, pp. 1131–1144, Dec. 1989.

[9] C. C. Chiu and Y. W. Kiang, "Electromagnetic imaging for an imperfectly conducting cylinder," *IEEE Trans. Microwave Theory Tech.,* vol. 39, pp. 1632–1639, Sept. 1991.

[10] F. Hettlich, "Two methods for solving an inverse conducting scattering problem," *Inverse Problems,* vol. 10, pp. 375–385, 1994.

[11] M. M. Ney, A. M. Smith, and S. S. Stuchly, "A solution of electromagnetic imaging using pseudoinverse transformation," *IEEE Trans. Med. Imag.,* vol. 3, pp. 155–162, Dec. 1984.

[12] W. Wang and S. Zhang, "Unrelated illumination method for electromagnetic inverse scattering of inhomogeneous lossy dielectric bodies," *IEEE Trans. Antennas Propagat.,* vol. 40, 1292–1296, Nov. 1992.

[13] S. Caorsi, G. L. Gragnani, and M. Pastorino, "Numerical electromagnetic inverse-scattering solutions for two-dimensional infinite dielectric cylinders buried in a lossy half-space," *IEEE Trans. Microwave Theory Tech.,* vol. 41, pp. 352–356, Feb. 1993.

[14] D. Colton and P. Monk, "A modified dual space method for solving the electromagnetic inverse scattering problem for an infinite cylinder," *Inverse Problems,* vol. 10, pp. 87–107, 1994.

[15] N. Joachimowicz, C. Pichot, and J. P. Hugonin, "Inverse scattering: an iterative numerical method for electromagnetic imaging," *IEEE Trans. Antennas Propagat.,* vol. 39, pp. 1742–1752, Dec. 1991.

[16] G. P. Otto and W. C. Chew, "Inverse scattering of H_z waves using the local shape-function imaging: a T-matrix formulation," *Int. J. Imag. Syst. Technol.,* vol. 5, pp. 22–27, Jan. 1994.

[17] R. F. Harrington, *Field Computation by Moment Methods.* New York: Macmillan, 1968.

[18] A. Ishimaru, *Electromagnetic Wave Propagation, Radiation and Scattering.* Englewood Cliffs, NJ: Prentice-Hall, 1991.

[19] J. H. Richmond, "TE-wave scattering by a dielectric cylinder of arbitrary cross-section shape," *IEEE Trans. Antennas Propagat.,* vol. 14, pp. 460–464, July 1966.

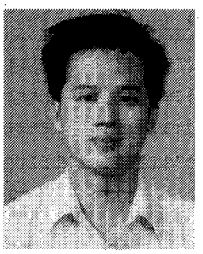

Chien-Ching Chiu was born in Taoyuan, Taiwan, Republic of China, on January 23, 1963. He received the B.S.C.E. degree from National Chiao Tung University, Hsinchu, Taiwan, in 1985 and the M.S.E.E. and Ph.D. degrees from National Taiwan University, Taipei, Taiwan, in 1987 and 1991, respectively.

From 1987 to 1989, he served in the ROC Army Force as a Communication Officer. In 1992, he joined the faculty of the Department of Electrical Engineering, Tamkang University, where he is now an Associate Professor. His research interest include microwave imaging, numerical techniques in electromagnetics, and indoor wireless communications.

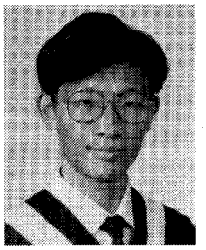

Po-Tsun Liu was born in Tainan, Taiwan, Republic of China, on September 13, 1971. He received the B.S. degree in physics from Tamkang University, Tamsui, Taiwan, in 1994. He has been working toward the master degree at the Department of Electrical Engineering, Tamkang University.

His current research interests include microwave imaging and numerical techniques in electromagnetics.